Solar Energy Materials & Solar Cells 94 (2010) 1953–1958

Contents lists available at ScienceDirect

Solar Energy Materials & Solar Cells

journal homepage: www.elsevier.com/locate/solmat

Band structure at heterojunction interfaces of GaInP solar cells

A.S. Gudovskikh [a,*], J.P. Kleider [b], N.A. Kalyuzhnyy [c], V.M. Lantratov [c], S.A. Mintairov [c]

[a] Saint-Petersburg Physics and Technology Centre for Research and Education of the Russian Academy of Sciences, Hlopina Street 8/3, 194021 St. Petersburg, Russia
[b] LGEP, CNRS UMR 8507, SUPELEC, Univ Paris-Sud, UPMC Univ Paris 06, 11 rue Joliot-Curie, Plateau de Moulon, F-91192 Gif-sur-Yvette Cedex, France
[c] A.F. Ioffe Physical-technical Institute, Polytechnicheskaya Street 26, 194021 St.-Petersburg, Russia

ARTICLE INFO

Article history:
Received 18 November 2009
Received in revised form
21 June 2010
Accepted 25 June 2010
Available online 14 July 2010

Keywords:
III/V Solar cells
Interfaces
Heterojunction

ABSTRACT

Experimental study of the band structure at the heterojunction interfaces of GaInP solar cells was performed by admittance spectroscopy. Admittance measurements were analyzed using numerical simulations. A good agreement between simulation and experiment was obtained. A potential barrier of about 0.6 eV at the p-GaAs/p-AlInP interface formed due to the high valence band offset was observed by the experiment. This high barrier creates fundamental limitation for the usage of this interface in p–n GaInP solar cells. A way to reduce the effective barrier height to 0.25 ± 0.02 eV using a double layer p-AlGaAs/p-AlGaInP window avoiding deterioration of *I–V* curves was demonstrated.

1. Introduction

The III–V multijunction solar cells allow one to achieve the highest efficiency, more than 41% [1,2]. These devices consist of many layers, including a large number of interfaces between different types of materials like III-arsenides (GaAs, AlGaAs) and III-phosphides (GaInP, AlInP). Therefore, the role of interfaces should be taken into account in the development of such devices. For instance, a significant role of interfaces in GaInP top sub-cell was demonstrated [3]. The band structure at interfaces is also a very important issue in any heterojunction device. In solar cells, band discontinuities can be either an advantage when producing a high potential barrier for minority carriers (like in back surface fields or window layers) or a drawback when forming undesired potential barriers for majority carriers that result in significant losses. The influence of interface band structure on GaInP solar cell performance was discussed in a previous paper [4]. It was supposed that the high value of the valence band offset at the p-GaAs/p-AlInP interface placed at the front contact of p- on n-type (hereafter, p–n) GaInP solar cells leads to the formation of high potential barriers for the holes, resulting in a knee on *I–V* curves. The knee on *I–V* curves for p–n GaInP solar cells and the subsequent deterioration of solar cell performance were observed by other authors [3,5]. This fact limits the application of p–n GaInP solar cells, resulting in the usage of n–p GaInP top sub-cell in high efficiency triple-junction solar cells. However p–n GaInP solar cells formed on n-type GaAs substrate are essential, for example, in mechanically stacked solar cells due to the significantly lower absorption in the IR region compared with p-type GaAs substrates. Therefore a way to improve the quality of p–n GaInP solar cells is still an actual task.

In our previous works the analysis of the influence of the band structure at the interfaces in GaInP solar cells on *I–V* curves was made using numerical modelling based on literature data on band discontinuities [4,5]. In this paper an experimental study of the band structure at the heterojunction interfaces using admittance spectroscopy is presented. Confirmation of the simulation results by experimental data is necessary for further analysis and development.

2. Theory

Experimental study of the band structure was made using admittance spectroscopy. This technique is based on measurements of capacitance and conductance versus temperature and frequency. Admittance spectroscopy is a powerful tool for studying bulk defect states [7,8], interface states [9] and band discontinuities in quantum well heterojunction structures [10]. Commonly, admittance data analysis is based on the capture and emission process of the charge carriers at and from the electronic states. Another approach to admittance spectroscopy analysis may be applied, which is related to the transport limitation across heterointerfaces. This approach based on the temperature dependence of the conductance is used here and allows us to determine the effective potential barriers for the majority carriers.

A scheme and schematic presentation of the band diagram of p–n GaInP solar cell with p-AlInP window layer are shown in

* Corresponding author. Tel.: +7 812 4486980; fax: +7 812 534 58 50.
E-mail address: gudovskikh@edu.ioffe.ru (A.S. Gudovskikh).

0927-0248/$ - see front matter © 2010 Elsevier B.V. All rights reserved.
doi:10.1016/j.solmat.2010.06.027

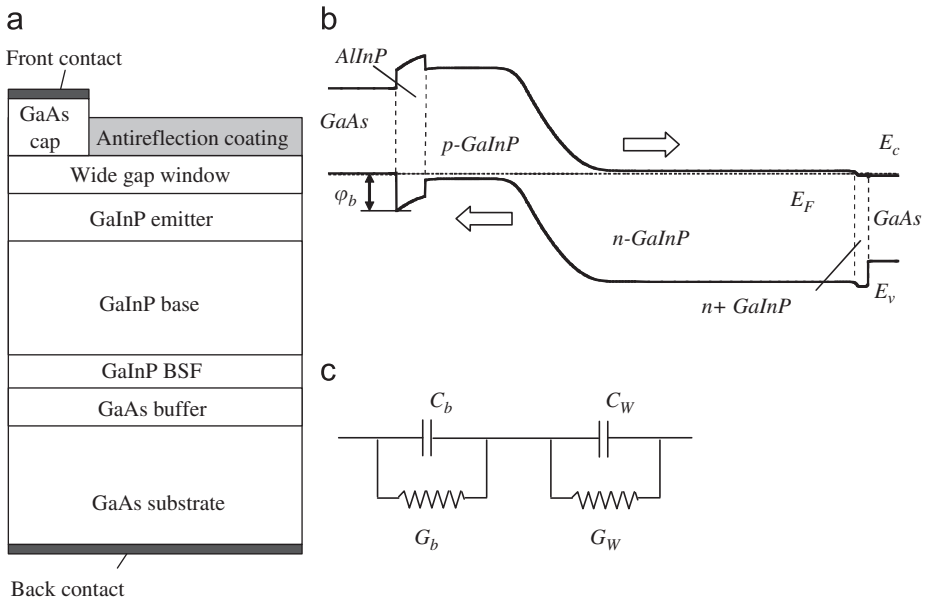

Fig. 1. Scheme of the GaInP solar cell (a). Schematic band diagram for p–n structure with p-AlInP window (b) and proposed equivalent circuit (c).

Fig. 1a and b. A GaAs cap layer is required to form front ohmic contact to the solar cell. A high potential barrier is supposed to be formed at the top interface between p-GaAs cap and p-AlInP window layers due to the high valence band offset, leading to the depletion of the AlInP layer [3]. No other barriers for the photo-generated charge carrier transport are expected from the band diagram (Fig. 1b). The simplest analysis of the admittance spectra may be made in terms of the equivalent circuit. The corresponding equivalent circuit is shown in Fig. 1c, where C_W and G_W are the capacitance and conductance of the depletion region of the p–n junction in GaInP, respectively, while C_b and G_b are those of the depletion region formed at the GaAs/AlInP and AlInP/GaInP interfaces.

Neglecting the conductance of the p–n junction G_W the equivalent parallel capacitance, C_p, and conductance, G_p, are equal to

$$C_p = \frac{C_W G_b^2 + \omega^2 C_W C_b (C_W + C_b)}{G_b^2 + \omega^2 (C_W + C_b)^2}, \quad (1)$$

$$G_p = \frac{\omega^2 C_W G_b}{G_b^2 + \omega^2 (C_W + C_b)^2}, \quad (2)$$

where ω is the angular frequency. Assuming that G_b is mostly related to hole transport through the potential barrier it may be expressed in terms of thermionic emission as follows:

$$G_b = G_0 \exp\left(\frac{-q\varphi_b}{kT}\right), \quad (3)$$

where G_0 is the temperature dependent thermoionic emission pre-factor, q the electron charge, φ_b the effective height of the potential barrier, k is Boltzmann's constant and T is temperature.

The calculated temperature dependences of C_p and G_p/ω, using formulas (1)–(3) with temperature independent values of C_W, C_b and G_0 for different frequencies, are presented in Fig. 2. Capacitance curves exhibit a step accompanied by a maximum in conductance. An Arrhenius plot of the measurement frequency at the conductance maximum (also corresponding to the inflection point in the capacitance) gives an activation energy equal to the potential barrier height φ_b (0.6 eV) used in the calculations. We should note that the determined value of φ_b is an effective barrier height, which may be less than that of the potential barrier due to the tunneling through the upper part of the barrier. Therefore the case where the barrier is transparent by tunneling (e.g. heavy doped material) cannot be determined by the proposed technique.

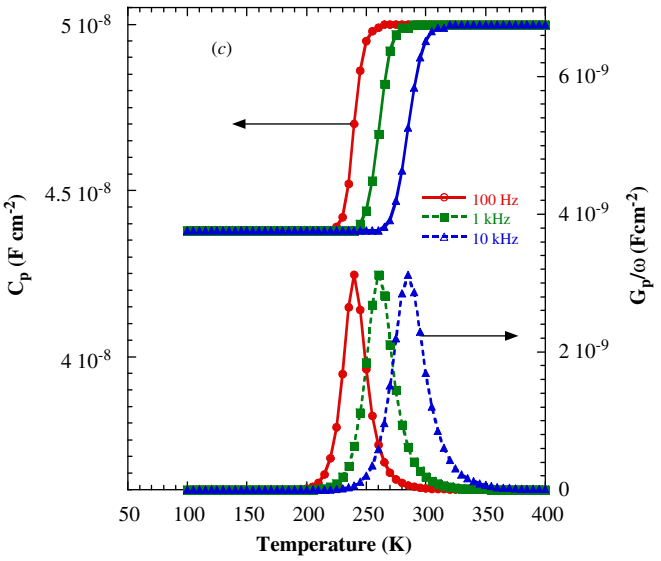

Fig. 2. Calculated curves of C_p and G_p/ω versus temperature (C) for 100 Hz, 1 kHz and 10 kHz using $C_W = 5 \times 10^{-8}$ F cm^{-2}, $C_b = 3.5 \times 10^{-7}$ F cm^{-2}, $G_0 = 10^9\ \Omega^{-1}$ cm^{-2} and $\varphi_b = 0.6$ eV.

This simple model demonstrates the way for the direct determination of the effective potential barrier height using admittance spectroscopy. For the determination of the barrier height from the experimental data the different sources of errors like the temperature dependence thermoionic emission pre-factor G_0 should be taken into account.

3. Experiment

Samples of $Ga_{0.48}In_{0.52}P$ (hereafter, GaInP) solar cells with $Al_{0.47}In_{0.53}P$ (hereafter, AlInP) and $Al_{0.8}Ga_{0.3}As/(Al_{0.3}Ga_{0.7})_{0.51}In_{0.49}P$ (hereafter, AlGaAs/AlGaInP) window were grown by MOVPE. The p–n GaInP heterostructures on n-GaAs substrate with

Si-doped (10^{18} cm^{-3}) n-GaAs buffer layer (150 nm), Si-doped (10^{18} cm^{-3}) BSF n-GaInP layer (50 nm), Si-doped (10^{17} cm^{-3}) n-base GaInP layer (920 nm), undoped GaInP layer (100 nm), Zn-doped (10^{18} cm^{-3}) p-emitter GaInP layer (30 nm) and Zn-doped (10^{17} cm^{-3}) p-AlInP (30 nm) or double layer (10^{18}/10^{18} cm^{-3}) p-$Al_{0.8}Ga_{0.3}As$/p-$(Al_{0.3}Ga_{0.7})_{0.51}In_{0.49}P$ (15/15 nm) p-window layer followed by Zn-doped (10^{19} cm^{-3}) cap p-GaAs (300 nm) contact layer were grown. For comparison, n–p GaInP heterostructures on p-GaAs substrate with Zn-doped (10^{18} cm^{-3}) p-GaAs buffer layer (150 nm), Zn-doped (10^{18} cm^{-3}) BSF p-GaInP layer (50 nm), Zn-doped (10^{17} cm^{-3}) p-base GaInP layer (800 nm), Si-doped (10^{18} cm^{-3}) n-emitter GaInP layer (50 nm) and Si-doped (10^{18} cm^{-3}) n-AlInP window layer (30 nm) followed by Si-doped (10^{18} cm^{-3}) cap n-GaAs contact layer (300 nm) were grown. AgMn:Ni:Au and AuGe:Ni:Au were used as contact electrodes on p-GaAs and n-GaAs, respectively. Contact grid and ZnS/MgF_2 antireflection coating were formed on the top of 3.2×8.3 mm^2 size solar cells. Heavily doped GaAs cap layer grown on the top of the heterostructures for ohmic contact formation was etched in the photoactive area before antireflection coating deposition. Special mesa structures with full coverage of metal top contact of 0.9 mm diameter were fabricated for admittance measurements.

I–V curves of the solar cells were measured at one sun AM1.5D illumination condition. The experimental admittance measurements were performed on mesa structures in a liquid nitrogen cryostat in the temperature range 90–350 K and frequency range 25 Hz–1 MHz.

Band diagrams and *I–V* curves of the solar cells and admittance spectra of the mesa structures were simulated using AFORS-HET 2.2 software [11]. Values of the band gap (E_g) and of the electron affinity (χ) used in the simulation are derived from the literature [12–17] and presented in Table 1. These values also determine that of the band offsets according to Anderson's approach [18]. For more simulation details refer to [4].

4. Results and discussion

The experimental *I–V* curve of GaInP p–n solar cell with p-AlInP window under AM1.5D illumination is presented in Fig. 3a. The *I–V* curve has a pronounced knee near open circuit voltage, V_{OC}, resulting in the reduction of fill factor, *FF*, and V_{OC} values. This behavior was suggested to be caused by the high potential barriers for the holes in the p-region, which is formed due to the high value of the valence band offset, ΔE_v, at the p-GaAs/p-AlInP interface [4]. This suggestion was derived from simulations based on literature data on band discontinuity values, which were not supplied by direct measurements. The results of admittance measurements presented in Fig. 3b demonstrate the presence of the potential barrier in this structure.

The activation energy obtained from an Arrhenius plot, which corresponds to the effective barrier height, is equal to 0.6 eV. As can be seen from the calculated band diagram (Fig. 4a) the height of the potential barrier corresponds to the value of ΔE_v at p-GaAs/p-AlInP interface because of high doping level of the p-GaAs layer. The obtained value of activation energy is in good agreement with the values of ΔE_v at the p-GaAs/p-AlInP interface reported in the literature [15]. The value $\Delta E_v = 0.63$ eV was used for the simulation of $C(T,f)$ and $G/\omega(T,f)$ using AFORS-HET software (see Fig. 4b). The behavior of the simulated curves corresponds well to that of the experiment and the same activation energy of 0.6 eV was extracted from the Arrhenius plot. The value of the activation energy corresponds to the barrier height, being equal to the difference between the energy of the Fermi level and the valence band of AlInP at the interface. This value is somewhat less than ΔE_v because of slight band bending in GaAs. The *I–V* curve under illumination was simulated using $\Delta E_v = 0.63$ eV (Fig. 3a). The simulated *I–V* curve also reproduces quite well the specific feature of the experimental one.

For comparison an example of the *I–V* curves of the n–p GaInP solar cells with n-AlInP window measured under AM1.5D

Table 1
Values of the band gap (E_g), the electron affinity (χ) of the layers as well as band gap offsets (ΔE_C, ΔE_V) values of different interfaces used in the simulations are presented.

Material	E_g (eV)	χ (eV)	Interface	ΔE_C (eV)	ΔE_V (eV)
GaAs	1.42 [10]	4.07 [10]	GaAs/AlInP	0.3	0.63
$Ga_{0.52}In_{0.48}P$	1.85 [11]	4.01 [14]	GaInP/AlInP	0.23	0.27
$Al_{0.53}In_{0.47}P$	2.35 [12]	3.78 [14]	GaAs/AlGaAs	0.54	0.13
$Al_{0.8}Ga_{0.2}As$	2.09 [13]	3.53 [15]	GaInP/AlGaInP	0.12	0.16
$(Al_{0.3}Ga_{0.7})_{0.51}In_{0.49}P$	2.13 [13]	3.89 [13]	AlGaAs/AlGaInP	0.35	0.39

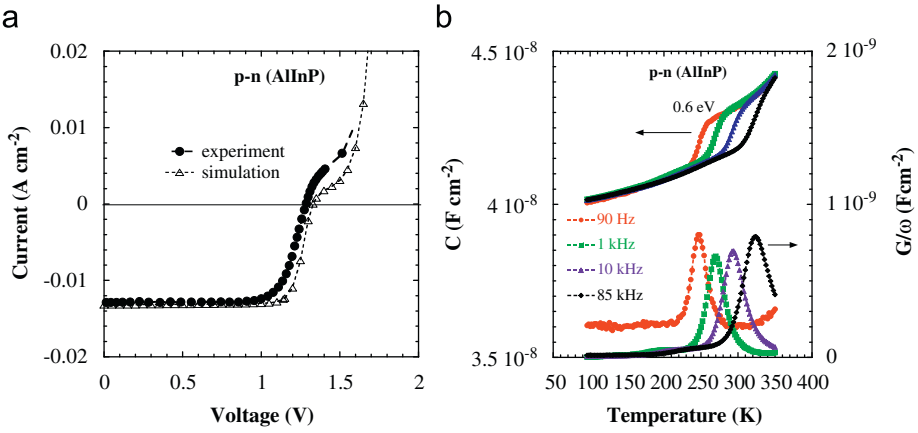

Fig. 3. Experimental and simulated *I–V* curve of GaInP p–n solar cell with p-AlInP window under AM1.5D illumination (a). Experimental $C(T,f)$ and $G/\omega(T,f)$ curves measured on the mesa structures, which were made on the same wafer (b).

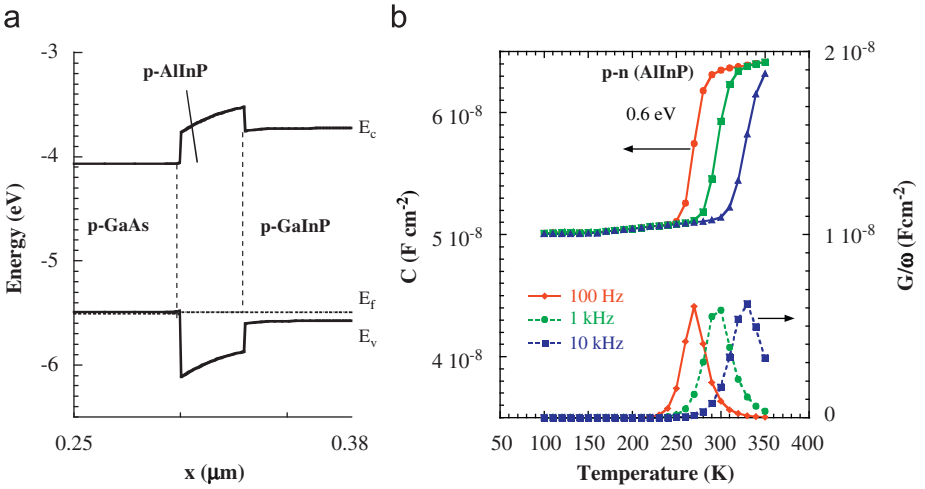

Fig. 4. Calculated band diagram of the top interfaces of GaInP p–n structure with p-AlInP window (a). $C(T,f)$ and $G/\omega(T,f)$ curves simulated with AFORS-HET 2.2 for the same structure (b).

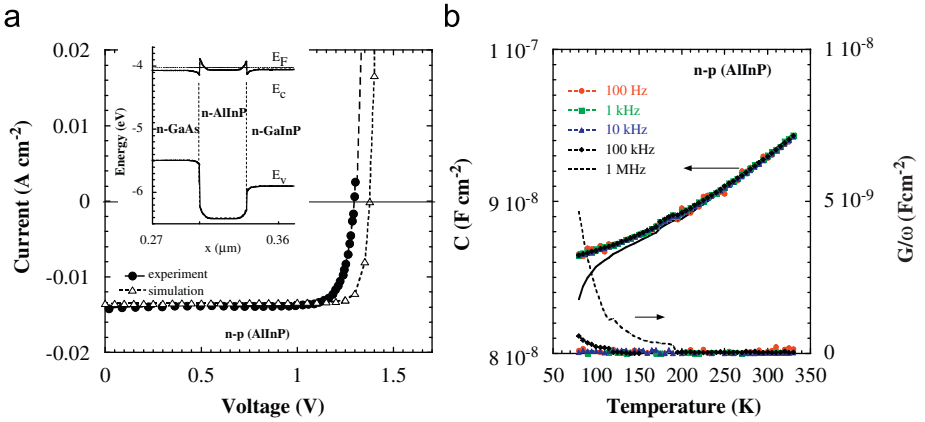

Fig. 5. Experimental and simulated *I–V* curve of GaInP n–p solar cell with n-AlInP window under AM1.5 illumination (a). Calculated band diagram of the top interfaces is shown in the inset. Experimental $C(T,f)$ and $G/\omega(T,f)$ curves measured on the mesa structures (b).

illumination is presented in Fig. 5a. The *I–V* curve does not exhibit any knee. From the calculated band diagram of this structure (inset of Fig. 5a) no significant potential barriers are expected to be overpassed by the electrons at the window interfaces. The admittance measurements are in agreement with the calculated band diagram. No step (peak) can be observed in the explored range of temperature and frequency (Fig. 5b). Only at the highest measured frequency (1 MHz) the $C(T)$ and $G/\omega(T)$ curves exhibit some feature at low temperature, which could be related to the existence of a step in capacitance and peak in conductance that could be revealed at lower temperature. This means that the activation energy related to the effective barrier height is too small to be determined in the given range of temperature and frequency as was predicted from the calculated band diagram, where the maximum barrier height of 0.2 eV may be estimated (without taking into account tunneling effect). The *I–V* curves, simulated using the proposed band diagram, do not exhibit any knee, in good agreement with the experiment (Fig. 5a).

Thus, it was experimentally demonstrated that the presence of a knee in *I–V* curves of the p–n GaInP solar cells is caused by the high potential barrier for majority carriers at the p-GaAs/p-AlInP interface. Therefore, to improve the performance of p–n GaInP solar cells another p-type window, which does not form a significant barrier for the holes, should be found.

One of the best candidates for p-window is the AlGaAs alloy, which does not form a significant potential barrier for the holes at the p-GaAs/p-AlGaAs interface due to the low value of the valence band offset. The p–n GaInP solar cells with p-$Al_{0.8}Ga_{0.2}As$ window do not exhibit any knee in *I–V* curves [6]. But the band bending at the p-AlGaAs/p-GaInP interface leads to enhanced recombination at this interface, resulting in a decrease of solar cell efficiency [4]. The p-AlGaInP/p-GaInP interface has a lower band bending, leading to lower recombination rate at the interface states. It was suggested to combine the advantages of p-GaAs/p-AlGaAs and p-AlGaInP/p-GaInP interfaces using double layer window p-AlGaAs/p-AlGaInP [6]. The calculated band diagram of the top side of the junction with such double layer window is demonstrated in Fig. 6a. The barrier height for the holes (about 0.4 eV) is lower in this case compared with that for p-AlInP window (0.6 eV). According to the simulations of *I–V* curves under illumination this barrier height is low enough for normal hole transport at 300 K (Fig. 6b). No knee in *I–V* curves was also observed up to 1000 suns illuminations. The influence of defect states at the p-AlGaInP/p-GaInP interface on solar cell performance is not significant up to values of density of states of $10^{12}\,cm^{-2}\,eV^{-1}$. This is much better than that for the p-AlGaAs/p-GaInP interface, where a dramatic decrease was observed for values of density of states higher than $10^{9}\,cm^{-2}\,eV^{-1}$. A detailed analysis of the simulation results is presented elsewhere [6].

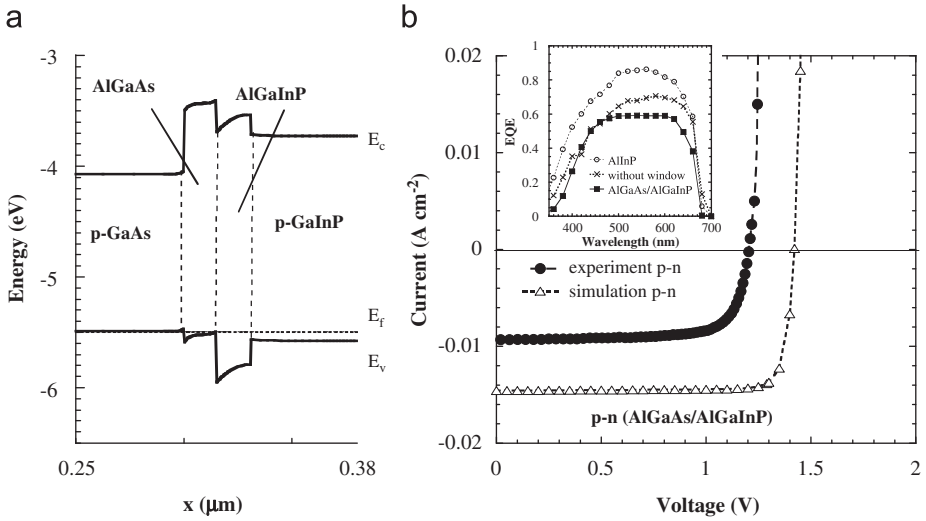

Fig. 6. Calculated band diagram of the top interfaces of GaInP p–n solar cell with p-AlGaAs/p-AlGaInP window (a). Experimental and simulated *I–V* curve of this solar cell under AM1.5D illumination (b). The experimental external quantum efficiency for p–n solar cells with p-AlInP, without and with p-AlGaAs/p-AlGaInP window are presented in inset.

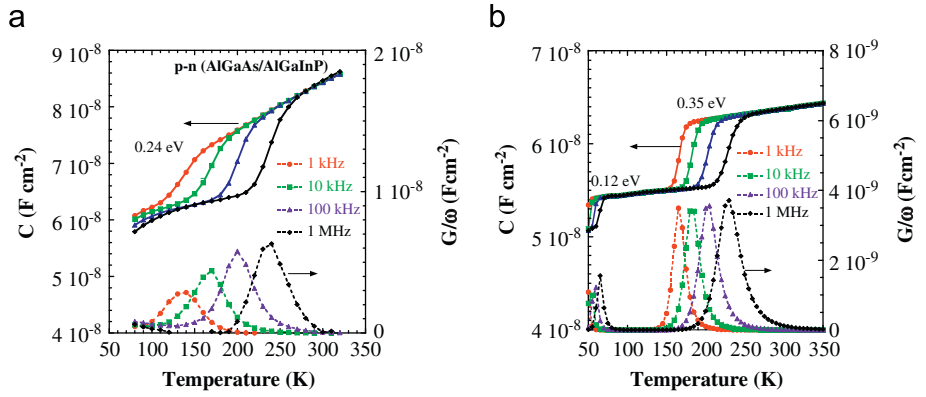

Fig. 7. Experimental $C(T,f)$ and $G/\omega(T,f)$ curves measured on p–n GaInP heterojunction with p-AlGaAs/p-AlGaInP window (a). $C(T,f)$ and $G/\omega(T,f)$ curves simulated with AFORS-HET 2.2 for the same structure (b).

The first experimental p–n GaInP heterostructure with p-AlGaAs/p-AlGaInP window was grown. Solar cells and mesa structures were fabricated on the basis of this heterostructure. The results of admittance measurements performed on mesa structures are shown in Fig. 7a. In the temperature range 120–220 K the capacitance has a step accompanied by a peak in conductance. The activation energy of this capacitance (conductance) step (peak) is in the range 0.23–0.27 eV. At lower temperature the capacitance and conductance seem to have another step and peak, respectively. The temperature and frequency limitation does not allow us to determine the activation energy of this low temperature step. However, the simulation of admittance spectra (Fig. 7b) predicts the presence of two steps (peaks). The step at low temperature corresponds to the transport over the barrier at the p-GaAs/p-AlGaAs interface with an activation energy of 0.12 eV related to this barrier height. The second step (peak) at higher temperature corresponds to the transport over the barrier at the p-AlGaAs/p-AlGaInP interface with the activation energy of 0.35 eV. Thus the activation energy obtained from admittance measurements corresponds to the effective barrier height of the AlGaAs/AlGaInP interface. The lower value of activation energy obtained from the experiment compared to the simulation may be caused by tunneling through the spike in the valence band. Of greatest importance, the obtained experimental value of effective barrier (0.25 ± 0.02 eV) should be low enough to ensure good transport of the majority carriers.

In Fig. 6b the experimental *I–V* curve of the p–n GaInP solar cell with p-AlGaAs/p-AlGaInP window is presented. No knee may be observed in this *I–V* curve as well as for *I–V* curves up to 150 suns (experiment limit). However, the absolute values of the short circuit current and open circuit voltage are significantly lower compared with those obtained for other structures and from simulations. This is expected to be due to the low diffusion length in the GaInP layers in this structure as can be seen from the spectral dependence of external quantum efficiency, EQE (see inset of Fig. 6b). EQE for p–n solar cells with p-AlGaAs/p-AlGaInP window is significantly lower at long wavelength range compared with that of the cell with p-AlInP window. Moreover EQE for the double window layer cell is even lower than that of the cell without window layer, where recombination at the front contact is not limited by any barrier. Therefore the poor performance of the double window layer solar cells is not related only to recombination at the front interface. New series of the p–n GaInP solar cells with p-AlGaAs/p-AlGaInP window should be made in the future. Nevertheless, experimental confirmation of the double layer window approach was demonstrated.

5. Conclusion

The capabilities of admittance spectroscopy to study the band structure at the heterojunction interfaces of GaInP solar cells were demonstrated by experiment and simulations. Admittance measurements allow one to estimate the effective barrier height for the majority carriers. In particular, experimental confirmation of the potential barrier of 0.6 eV at the p-GaAs/p-AlInP interface was obtained. It was shown that this barrier formed due to the high value of the valence band offset, causing the knee in *I–V* curves of the p–n GaInP solar cells. A way to avoid the knee in *I–V* curves of the p–n GaInP solar cells is to reduce the effective barrier height to 0.25 ± 0.02 eV using a double layer p-AlGaAs/p-AlGaInP window.

Acknowledgments

This work was supported by the Russian Foundation for Basic Research under Grant # 08-08-00916-a, as well as by CNRS in the framework of a joint Russian–French PICS Project and by NATO Reintegration Grant NR.RIG 982984. A.S. Gudovskikh would like to thank the Council on Grants of the President of the Russian Federation for Grant # MK-71.2009.8.

References

[1] W. Guter, J. Schöne, S.P. Philipps, M. Steiner, G. Siefer, A. Wekkeli, E. Welser, E. Oliva, A.W. Bett, F. Dimroth, Current-matched triple-junction solar cell reaching 41.1% conversion efficiency under concentrated sunlight, Appl. Phys. Lett. 94 (22) (2009) 223504/1–223504/3.

[2] R.R. King A. Boca, W. Hong, D. Larrabee, K.M. Edmondson, D.C. Law,C.M. Fetzer, S. Mesropian N.H. Karam, Band-gap-engineered architectures for high-efficiency multijunction concentrator solar cells, in: Proceedings of the 24th European Photovoltaic Solar Energy Conference, Hamburg, Germany, September 21–25, 2009, pp. 55-61.

[3] S.R. Kurtz, J.M. Olson, D.J. Friedman, J.F. Geisz, K.A. Bertness, A.E. Kibbler, Passivation of interfaces in high-efficiency photovoltaic devices, in: H. Hasegawa, M. Hong, Z.H. Lu, S.J Pearton (Eds.), Compound Semiconductor Surface Passivation and Novel Device Processing, Materials Research Society Symposium Proceeding Volume 573, Warrendale, 1999, pp. 95–106.

[4] A.S. Gudovskikh, N.A. Kaluzhniy, V.M. Lantratov, S.A. Mintairov, M.Z. Shvarts, V.M. Andreev, Numerical modelling of GaInP solar cells with AlInP and AlGaAs windows, Thin Solid Films 516 (2008) 6739–6743.

[5] Steven I. Wojtczuk, Stanley M. Vernon, Michael M. Sanfacon, Comparison of windows of p-on-n InGaP solar cells, Proceedings of the 23rd IEEE Photovoltaic Specialists Conference (1993) pp. 655–658. doi:10.1109/PVSC.1993.347015.

[6] A.S. Gudovskikh, N.A. Kalyuzhnyy, V.M. Lantratov, S.A. Mintairov, M.Z. Shvarts, V.M. Andreev, Properties of interfaces in GaInP solar cells, Semiconductors 43 (10) (2009) 1363–1368.

[7] J.F. Chen, N.C. Chen, P.Y. Wang, H. Tsai, Electrical characteristics and deep-level admittance spectroscopies of low-temperature grown GaAs p-i-n structures, J. Appl. Phys. 81 (1997) 1255–1258.

[8] N.D. Nguyen, M. Germain, M. Schmeits, B. Schineller, M. Heuken, Thermal admittance spectroscopy of Mg-doped GaN Schottky diodes, J. Appl. Phys. 90 (2001) 985–993.

[9] P. Krispin, Single-level interface states in semiconductor structures investigated by admittance spectroscopy, Appl. Phys. Lett. 70 (1997) 1432–1434.

[10] S. Anad, N. Carlsson, M.E. Pistol, L. Samuelson, W. Seifert, Electrical characterization of InP/GaInP quantum dots by space charge spectroscopy, J. Appl. Phys. 84 (1998) 3747–3755.

[11] R. Stangl, M. Kriegel, M. Schmidt, AFORS-HET, version 2.2, a numerical computer program for simulation of heterojunction solar cells and measurements, in: Proceedings of the fourth World Conference on Photovoltaic Energy Conversion (WCPEC-4), Hawaii, USA, 2006, pp. 1350–1353.

[12] S.M. Sze, Physics of Semiconductor Devices, second ed., John Wiley & Sons, New-York, 1981, pp. 850–851.

[13] A. Gomyo, T. Suzuki, S. Iijima, Observation of Strong Ordering in $Ga_xIn_{1-x}P$ alloy semiconductors, Phys. Rev. Lett. 60 (1988) 2645–2648.

[14] D.P. Bour, J.R. Shealy, G.W. Wicks, W.J. Schaff, Optical properties of Al_x In_{1-x} P grown by organometaiUc vapor phase epitaxy, Appl. Phys. Lett. 50 (1987) 615–617.

[15] I. Vurgaftman, J.R. Meyer, L.R. Ram-Mohan, Band parameters for III–V compound semiconductors and their alloys, J. Appl. Phys. 89 (2001) 5815–5875.

[16] C.-S. Jiang, D.J. Friedman, H.R. Moutinho, M.M. Al-Jassim, Profiling the built-in electrical potential in III-V multijunction solar cells, Proceedings of the fourth World Conference on Photovoltaic Energy Conversion, Hawaii, USA, 2006, pp. 853–856.

[17] S. Adachi, GaAs, AlAs, and $Al_xGa_{1-x}As$: Material parameters for use in research and device applications, J. Appl. Phys. 58 (3) (1985) R1–R29.

[18] R.L. Anderson, Germanium–gallium arsenide heterojunction, IBM J. Res. Dev. 4 (3) (1960) 283–287.